J. Membrane Biol. 181, 77–89 (2001)
DOI: 10.1007/s00232-001-0011-7

The Journal of
Membrane
Biology

Modeling the Current-Voltage Characteristics of Charophyte Membranes. II.* The Effect of Salinity on Membranes of *Lamprothamnium papulosum*

M.J. Beilby, V.A. Shepherd
School of Physics, Biophysics, The University of NSW, Kensington 2052, NSW, Australia

Received: 27 January 2000/Revised: 19 January 2001

Abstract. *Lamprothamnium* is a salt-tolerant charophyte that inhabits a broad range of saline environments. The electrical characteristics of *Lamprothamnium* cell membranes were modeled in environments of different salinity: full seawater (SW), 0.5 SW, 0.4 SW, and 0.2 SW. The cells were voltage-clamped to obtain the *I/V* (current-voltage) and *G/V* (conductance-voltage) profiles of the cell membranes. Cells growing at the different salinities exhibited one of three types of *I/V* profiles (states): pump-, background- and K^+-states. This study concentrates on the pump- and background-states. Curved (pump-dominated) *I/V* characteristics were found in cells with resting membrane PDs (potential differences) of −219 ± 12 mV (in 0.2 SW: 6 cells, 16 profiles), −161 ± 12 mV (in 0.4 SW: 6 cells, 7 profiles), −151 ± 12 mV (in 0.5 SW: 6 cells, 12 profiles) and −137 ± 12 mV (in full SW: 8 cells, 13 profiles). The linear *I/V* characteristics of the background-state were found in cells with resting PDs of −107 ± 12 mV (in 0.4 SW: 7 cells, 12 profiles), −108 ± 12 mV (in 0.5 SW: 7 cells, 10 profiles) and −104 ± 12 mV (in full SW: 3 cells, 5 profiles). The resting conductance (*G*) of the cells progressively increased with salinity, from 0.5 $S{\cdot}m^{-2}$ (in 0.2 SW) to 22.0 $S{\cdot}m^{-2}$ (in full SW). The pump peak conductance only rose from 2 $S{\cdot}m^{-2}$ (0.2 SW) to 5 $S{\cdot}m^{-2}$ (full SW), accounting for the increasingly depolarized resting PD observed in cells in more saline media.

Upon exposure to hypertonic medium, both the pump and an inward K^+ rectifier were stimulated. The modeling of the *I/V* profiles identified the inward K^+ rectifier as an early electrical response to hypertonic challenge.

Key words: Salinity — *Lamprothamnium* — Current-voltage profiles — Pump model — Hypertonic effect.

Introduction

Many past civilizations collapsed because of progressive salinization of their land (e.g., Ashraf, 1994; Kerr, 1998). Nonetheless, increasing salinization of land in Australia and other parts of the world indicates that we have not come to grips with this problem. The problem can be addressed on many levels, and this is probably necessary for its ultimate solution. A detailed study of transport processes across cell membranes in salt tolerant plants, such as *Lamprothamnium papulosum*, will provide understanding of salt-tolerance at the cellular level.

Salt stress can be brought about by increasing soil salinity (often an effect of irrigation), drought and low temperatures. Salt stress is due both to osmotic stress and to the direct toxicity of increased cellular concentrations of Cl^- and Na^+ ions, which can perturb protein function. Even mild hypertonic stress can affect plant growth, which depends on turgor-driven stretching of the cell walls. Water is drawn out of a plant cell under salt stress, ultimately resulting in plasmolysis unless the cell can increase the concentration of its sap and cytoplasm. Experiments with charophytes show that the plasmalemma transport properties change irreversibly after plasmolysis, leading to high nonspecific conductance and cell death (Kourie & Findlay, 1990; McCulloch & Beilby, 1997). The irreversibility of the damage suggests that linkages between plasmalemma and cell wall are important for normal transport. Pickard and Ding (1993) propose that Ca^{++} channels contain such membrane-to-wall linkages.

Correspondence to: M.J. Beilby

* Sequel to Beilby and Walker, 1996, Modeling the current-voltage characteristics of *Chara* membranes: I. The Effect of ATP removal and zero turgor. *J Membrane Biol.,* 149:89–101

The plants that can cope with hyperosmotic stress use two mechanisms to increase the osmolarity of their contents: (i) uptake of inorganic ions, usually K^+, Cl^- and Na^+; (ii) synthesis of compatible solutes, such as sugars, polyols, amino acids or quaternary amines. Often both of these mechanisms are used, (i) being a rapid response which is modulated by (ii). The cytoplasmic compartment often utilizes (ii), as the concentrations of inorganic ions have to remain within narrow limits for many metabolic processes to function. Experiments on higher plant cells indicate that inorganic ions contribute between 50 and 100% of the osmotic adjustment in the vacuoles of bean mesophyll cells (Shabala, Babourina & Newman, 2000), maize (Cerda et al., 1995), wheat (Hu & Schmidhalter, 1998) and *Avicennia* (Suarez, Sobrado & Medina, 1998). Many types of plant cell respond to hypertonic shock by hyperpolarization of the membrane potential difference (PD) and increased proton extrusion (e.g., Shabala et al., 2000; Curti, Massardi & Lado, 1993 and references cited therein). Stimulation of the pump makes good sense from a thermodynamic point of view since hyperpolarization to PDs more negative than E_K (E = equilibrium PD) leads to an inward electrochemical gradient for K^+. K^+ is the major cation taken up or expelled during volume regulation by diverse animal, plant, and algal cells, or bacteria (Chamberlin and Strange, 1989). The opening of inward rectifying K^+ channels with pump activation has been observed in many experiments (e.g., in guard cells, Blatt, 1999; wheat protoplasts, Findlay et al. 1994; *Arabidopsis* protoplasts, Colombo & Cerana, 1991). The inward rectifying K^+ channels in guard cells are inhibited by low medium K^+ concentration, increase in cytoplasmic Ca^{++} concentration and increase in cytoplasmic pH (Thiel et al., 1993).

The Na^+ electrochemical gradient is directed inwards at normal resting PD, but highly Na^+ selective channels have not been observed in plants. Amtmann and Sanders (1999) reviewed recent experiments and modeled most likely mechanisms for Na^+ entry. While most inward rectifying channels tend to be selective for K^+, Tyerman et al. (1997) described a "spiky" inward rectifier in wheat root cortex protoplasts with high P_{Na}/P_K ratio (P = permeability). Recent studies also describe voltage-independent channels with high P_{Na}/P_K ratios (see Amtmann & Sanders, 1999, for references). The modeling showed conclusively that at high Na^+ concentration in the medium, Na^+ influx through both inward rectifiers and voltage-independent channels became significant (Amtmann & Sanders, 1999). Salt-tolerant plants move Na^+ from the cytoplasm, where it is toxic, into the vacuole. Na^+/H^+ antiport is thought to be responsible because the electrochemical gradient is directed from vacuole to cytoplasm (Blumwald & Gelli, 1997). The H^+ gradient is provided by H^+ pumps at the tonoplast.

The influx of Cl^- presents another problem, as hyperpolarization actually increases the outward driving force on this ion (E_{Cl} in many plant cells is near zero—*see*, for instance, Hope & Walker, 1975; Hedrich, Bush & Raschke, 1990). The Cl^- influx, therefore, needs to be coupled to a "downhill" process. Sanders (1980) showed that starvation of Cl^- led to a subsequent 2- to 4-fold increase in Cl^- influx in *Chara*. Later, Beilby and Walker (1981) measured the *I/V* (current/voltage) profiles for a $2H^+/Cl^-$ symporter in *Chara.* This transporter is likely to play an important role in hypertonic osmoregulation.

It is not known how the cells detect hypertonic exposure. Cosgrove and Hedrich (1991) found mechanosensitive channels in guard cells that opened upon exposure to hypotonic medium (increased turgor pressure). These channels might inactivate in hypertonic medium (decreased turgor pressure), initiating the signal cascade perhaps by smaller background current and concomitant hyperpolarization, which in turn could stimulate the proton pump. Another hypothesis suggests that the H^+ pump is the primary receptor in cells of *Senecio* leaf segments (Reinhold, Seiden & Volokita, 1984). However, Shabala et al. (2000, and references therein) found that inhibition of the proton pump in bean mesophyll cells did not abolish K^+ and Cl^- influx, but K^+-free medium prevented the pump stimulation. Thus, the inward K^+ rectifier seems to play an important role in the sensing of the hypertonic turgor decrease (Shabala et al., 2000; Liu & Luan, 1998).

Lamprothamnium is a salt-tolerant charophyte that is able to regulate turgor pressure of its cells, like guard cells, but unlike salt-sensitive freshwater *Chara* and plant cells such as bean mesophyll. Charophyte cells can provide special insights into fundamental mechanisms of the response to salinity changes in land plants. Cladistic analysis indicates that such charophytes may be living representatives of the group that gave rise to flowering plants (Bremer et al., 1987). Further evidence relating charophytes to land plants comes from analysis of chloroplast nucleic acids and morphology. Two chloroplast tRNA introns gained by charophytes and land plants is evidence of a genetic connection between ancient charophytes and today's land plants (Manhart & Palmer, 1990; Baldauf, Manhart & Palmer, 1990). The charophyte chloroplast also has grana, similarly to land plants, but unlike most other algae (Gunning and Schwartz, 1999). Although most living charophytes are freshwater organisms, it is likely that they have evolved from a salt-tolerant ancestor (Winter, Soulie-Marsche & Kirst, 1996).

Turgor-regulation has been intensively studied in the salt-tolerant charophyte, *Lamprothamnium.* After hyper-

tonic exposure the cells regulate their turgor pressure, $\Delta\pi$, to its setpoint of ~300 mosmol·kg^{-1} by importing K^+, Cl^- and Na^+ over many hours (Bisson & Kirst, 1980). The resting p.d. hyperpolarizes by more than 50 mV over 20 hours (Okazaki, Shimmen & Tazawa, 1984, Okazaki & Tazawa, 1990). The involvement of the proton pump was confirmed by using pump inhibitor DCCD (Okazaki, 1993). As the H^+ pump is stimulated and the same ions are accumulated as in land plants, we assumed that the K^+ inward rectifier and $2H^+/Cl^-$ symporter are present in the *Lamprothamnium* plasmalemma. Interestingly, the K^+ inward rectifier has not been observed in salt-sensitive charophytes, where the inward rectifying currents are carried by Cl^- outflow (Tyerman et al., 1986a,b). Such a transporter would deplete the cell's Cl^- upon hyperpolarization and it is, therefore, unlikely to reside in the plasmalemma of *Lamprothamnium.* This is one possible adaptation which may allow *Lamprothamnium* to survive in salinities deadly to freshwater *Chara.* The K^+ channel described in the response to hypotonic shock (Beilby & Shepherd, 1996) inactivates at PDs more negative than −150 mV and is unlikely to be responsible for K^+ influx during hypertonic shock. The $2H^+/Cl^-$ symporter was described in *Chara* (Beilby & Walker, 1981). The transport routes for Na^+ are yet to be identified.

In our past work we have described the *I/V* profiles of *Lamprothamnium* membranes in cells growing in a range of saline environments (Shepherd, Beilby & Heslop, 1999). In this study we model the *I/V* profiles to quantify the contributions of various transporters to membrane conductance as a function of medium salinity. We focus on the features of the proton pump, the background current and the inward rectifier. We also apply this approach to hypertonic challenge of cells growing in a relatively dilute medium.

Materials and Methods

Plant Material

Lamprothamnium papulosum was collected from three sites in the Tuggerah Lakes system, Central Coast, NSW: (i) a permanent full seawater (SW) site at Chain Valley Bay on Lake Macquarie, (ii) a 0.5 SW site, in a ditch leading to Lake Budgewoi, which could be diluted to 0.2 SW after heavy rain, and (iii) a 0.4 SW site at a lake on a golf course near Budgewoi. Salinities were measured on-site using a hand-held refractometer. The medium from Lake Macquarie had a salinity of 34 practical salinity units: the other salinities corresponded to fractions of this. The concentrations of major ions were measured with a Corning 410C flame photometer and Sherwood chloride analyzer Model 926. The cells were transferred to artificial media prior to experiments. Full SW and 0.5 SW cells survived best in the lab in a mixture of Lake Macquarie water/ditchwater and Ocean Nature artificial seawater. Ocean Nature medium has a lower Na^+ concentration (~307 mM) than the lake (~465 mM) resulting in a lower overall (350 mM) Na^+ concentration in the medium. The 0.4 and 0.2 SW media were diluted from a stock SW medium containing (in mM) 465 NaCl, 10 KCl, 10 $CaCl_2$ and 2 $NaHCO_3$, and were made up to reflect the concentrations of Na^+, K^+, Cl^- at the collection site (*see* Table 1). Cells flourished in these media for weeks to months. The plants exhibited great morphological plasticity: marine plants from Lake Macquarie were only about ten centimeters in total length with most mature cells 7–10 mm long, while plants from lower salinities reached heights of 50 cm to 1 m, with basal cells up to 10 cm long. The thickness of the extracellular mucilage varied according to position of the cell on the plant and the medium salinity, as described earlier (Shepherd, Beilby & Heslop, 1999).

Electrophysiology

The electrophysiology techniques were described in detail by Beilby and Shepherd (1996). Briefly, cells were kept for at least 2 weeks in the media before experiments. Selected cells were mounted in a grooved perspex chamber with three compartments and sealed with silicon grease (*see* Fig. 1; Beilby, Mimura & Shimmen, 1997). The chamber was lit from below with a fiber-optic light source, and cells were observed using a dissecting microscope with maximum magnification of 120 ×. Microelectrodes were filled with 0.5 M KCl. The inner microelectrode was inserted into the center of the cell, when this was possible, or into the streaming cytoplasm. In many cells we found no significant difference in the PD or the form of *I/V* curves when the microelectrode was in the streaming cytoplasm or the center of the cell. We regard the microelectrode placement as vacuolar, given that the vacuole occupies a larger part of the charophyte cell than does the cytoplasm (Beilby & Shepherd, 1996). Steady PDs were obtained after 30–40 min when the medium was refreshed by hand at regular intervals. Cells were compartment-voltage-clamped (Beilby *et al.,* 1997). The *I/V* characteristics were obtained by voltage-clamping the PD across the cell membrane to a bipolar staircase command, generated by an LSI 11/73 computer, with pulse-widths of 60 msec separated by 200 msec at the resting PD. The data-logging of each *I/V* scan took 8 sec (Beilby, 1990; Beilby & Shepherd, 1996). A chart-recorder (Riken-Denshii, Tokyo, Japan) was used to provide a continuous record of the cell PD throughout the experiments.

As the membrane PD was clamped at more hyperpolarized levels, the clamp current became unpredictable, increasing suddenly and irreversibly and often killing the cell. In many cells, this sensitivity to hyperpolarized PDs limited the extent of negative-going voltage-clamp to between −250 and −300 mV.

The Hypertonic Effect

To study the hypertonic effect, we selected a group of cells growing in a dilute environment (0.2 SW). The cells were transparent with minimal extracellular mucilage (~1 μm at most) and had very hyperpolarized PDs. They were exposed to 0.4 SW—doubling the concentration of the major ions. These cells showed much greater tolerance to being voltage-clamped at hyperpolarized PDs (down to −400 mV).

The Model

The whole-cell currents flowing across the plasmalemma or plasmalemma and tonoplast in series were modeled to avoid artefacts stemming from the current subtractions (Beilby & Walker, 1996). The "Two-state" HGSS model (Hansen et al., 1981) was employed to describe the *I/V* characteristics of the proton pump:

$$i_p = zFN\frac{k_{io}\kappa_{oi} - k_{oi}\kappa_{io}}{k_{io} + k_{oi} + \kappa_{io} + \kappa_{oi}} \quad (1)$$

where

$$k_{io} = k_{io}^{o}\, e^{\frac{zFV}{2RT}} \quad (1a)$$

$$k_{oi} = k_{oi}^{o}\, e^{-\frac{zFV}{2RT}} \quad (1b)$$

F,*R*,*T* have their usual meaning, *z* is the pump stoichiometry, which has been set to 1. *N* is a scaling factor ($= 2 \times 10^{-8}$) and *V* is the p.d. across the plasmalemma or across both plasmalemma and tonoplast. While the number of carrier states is likely to be greater than two, the model for the *I/V* analysis can be reduced to a pair of PD-dependent rate constants, k_{io}, k_{oi} (assuming a symmetric Eyring barrier) and PD-independent rate constants, κ_{io}, κ_{oi} (Hansen et al., 1981). As we are fitting the total membrane *I/V* relationship, there is insufficient information to describe higher-state models. The modeled pump current and conductance are shown as dotted lines in Figs. 1–6, parts *b* and *c*, respectively.

The background current was approximated by a linear profile with zero current at −100 mV:

$$i_{background} = g_{background}(V + 100) \quad (2)$$

In *Lamprothamnium* the experimental evidence for such a background current is confirmed by *I/V* profiles of cells in "leak" or "background" state. The modeled background current and conductance are shown as (dash-stippled lines (— - — - —) in Figs. 1–6, parts *b* and *c*, respectively.

The inward rectifier current plays an important role in the hypertonic effect in *Lamprothamnium* and is thought to be carried by an inflow of K^+ rather than outflow of Cl^-, observed in salt-sensitive *Chara* (Tyerman, Findlay & Paterson, 1986a,b). We have modeled this current with the Goldman-Hodgkin-Katz (GHK) equation multiplied by Boltzman distribution of the open probability $P_{o,irc}$ (Amtmann & Sanders, 1999):

$$i_{irc} = \frac{P_{o,irc}\, N_K P_K F^2 V([K^+]_i - [K^+]_o\, e^{-\frac{FV}{RT}})}{RT(1 - e^{-\frac{FV}{RT}})} \quad (3)$$

$$P_{o,irc} = 1 - \frac{1}{1 + e^{-\frac{zgF(V - V_{50})}{RT}}} \quad (4)$$

where $[K^+]_o$ and $[K^+]_i$ are the K^+ concentrations outside and inside the cell, respectively. $[K^+]_i$ was taken as 150 mM for cells in 0.2 SW and 100 mM for the other salinities (based on Okazaki et al., 1984), $[K^+]_o$ is given in Table 1. $N_K P_K$ stands for number of K^+ channels and their permeability and is treated as a single parameter, z_g is the number of gating charges and V_{50} is the half activation potential. The modeled i_{irc} and g_{irc} are shown as long-dashed lines (- - - - -) in Figs. 1–5, parts *b* and *c*, respectively.

Similarly, the outward rectifier was modeled by eqn. (3), multiplied by the open probability $P_{o,orc}$:

$$P_{o,orc} = \frac{1}{1 + e^{-\frac{zgF(V - V_{50})}{RT}}} \quad (5)$$

The modeled i_{orc} and g_{orc} are shown as short-dashed lines (-------) in Figs. 1–5, parts *b* and *c*, respectively.

Table 1. Media

Medium	Na^+ mM	K^+ mM	Cl^- mM	Osmolarity mosmol kg^{-1}
Full SW	350	16	400	1072
0.5 SW	175	8	201	536
0.4 SW	154	4.1	172	281
0.2 SW	77	2.0	86	140.5

Only the main ions are given for each medium. *See* Methods for full explanation. Full SW was a mixture of Lake Macquarie water and Ocean Nature artificial medium. 0.5 SW was a mixture of ditch water and Ocean Nature medium. 0.4 SW and 0.2 SW were simplified media based on concentrations of Na^+, Cl^- and K^+ found at the collection sites. The pH self-buffered at pH 8.

The application of the Boltzmann distribution probability requires that the open and shut channel populations reach equilibrium at each membrane PD. The clamp currents at PDs more negative than −150 mV exhibited a fast relaxation (completed after ~50 ms), followed by a more gradual drift. In practice it was not possible to gather data after the slow current relaxation was completed. If the cells were clamped at negative levels for 8–15 sec, complex responses were observed. Some cells exhibited negative-going transients (probably due to Cl^- channels) and most cells showed unpredictable and irreversible large currents (as discussed in the previous section). The fast current relaxation was therefore taken as an indication of the channel populations adjusting to the new PD: a quasi-equilibrium. In the experiment monitoring the hypertonic effect, the time-dependence of the fast current relaxation was similar in all the *I/V* profiles. The fitting of the outward rectifier is also preliminary, as only a few points were available in the data sets (*see* Figs. 1 and 2). The rectifier modeling will be refined in future work.

The modeling of the data was performed on a Compaq Armada E500 notebook computer, using Mathematica 3.0. The goodness of fit was judged by eye. The conductance profiles (part *c* of all the figures) were obtained by differentiating the modeled currents.

Results

Steady-State *I/V* Profiles in the Range of Salinities 0.2 SW to Full SW

The cells in the ditch habitat experience the greatest fluctuations in salinity. After a period of rain, the ditch water had a comparatively low salinity (0.2 SW). Cells growing at this site, and transferred to the simplified 0.2 SW medium (Table 1), displayed hyperpolarized PD of −219 ± 12 mV (6 cells, 16 profiles) and low conductance (*see* Fig. 1*a* and *c*). The parameter values used to fit the data (*see* Fig. 1*b*) are given in Table 2. All the cells in this group were hyperpolarized, that is, in a pump-state, and none were in the spontaneous background- or leak-state. The most positive PD of the *I/V* profile was −100 mV, as the cells were excitable. Note the appearance of the outward rectifier between −150 and −100 mV. This is reflected by a more negative V_{50} than those in cells growing in more saline media (*see* Table 2). The inward rectifier exhibits a rather gradual increase with the PD

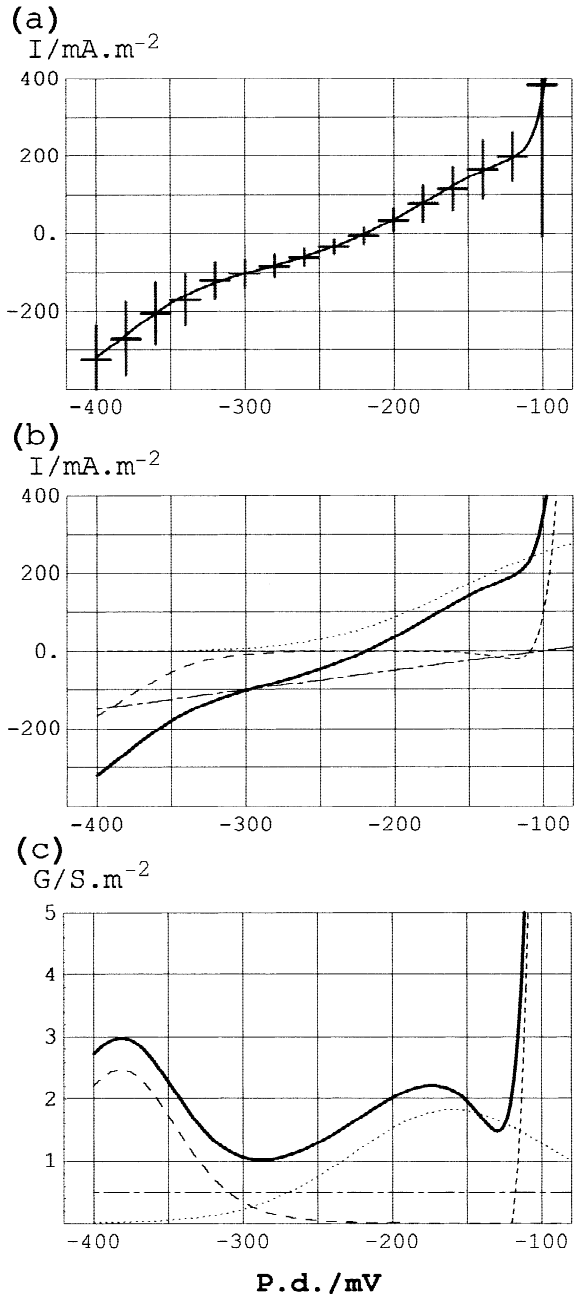

Fig. 1. (*a*) A set of 6 cells, 16 profiles, grown in 0.2 SW. The data have been gathered into 20 mV slots (horizontal error bars) and the standard errors are shown as the vertical bars. The line represents the total *I/V* profile generated by the model. The resting p.d. is given in Table 2. (*b*) The transport systems constituting the *I/V* profile: ····· the pump, — · — · — the background current, -------- the inward rectifier i_{irc}, - - - - the outward rectifier i_{orc}. For the mathematical forms see the Methods. The parameter values can be found in Table 2. The maximum clamp PD was limited to −100 mV to avoid excitation transients. (*c*) The corresponding *G/V* profiles.

going more negative. This is reflected by a low $N_K P_K$ compared to those in cells growing in more saline media (*see* Table 2). Compare also the magnitude of g_{irc} between −200 and −250 mV in Figs. 1–5, part *c*.

The cells grown in 0.4 SW (habitat iii) exhibited either the pump-state, with resting PD of −161 ± 12 mV (6 cells, 7 profiles), or the linear background-state with PD of −107 ± 12 mV (7 cells, 12 profiles). Both states are shown in Fig. 2*a*. The pump-state data are depicted by thick line error bars fitted by a thick line total current, while the background-state data are shown as thin line error bars, fitted by a thin line. The cells were much less excitable than those in the lower salinity, particularly the ones in the background-state. The apparent lower pump-state currents at 0 mV are due to opening of the excitation channels, which move the *I/V* baseline in the negative direction (Beilby, 1990). The currents fitted to the pump-state and the resulting conductances are given in 2*b* and *c*, respectively. The parameter values are given in Table 2. The outward rectifier appears between −50 and 0 mV (V_{50} = + 50 mV). The background-state data were modeled with a background current, no rectifiers and a small contribution from the pump, which is not shown (*see* parameters in Table 2). Only the total current and conductance are shown (thin line) in Fig. 2*b* and *c*, respectively. Note that the total background-state current and conductance closely coincide with the fitted background current and conductance of the pump-state (Fig. 2*b* and *c*).

The cells grown in the 0.5 SW (the ditch habitat, after long periods of evaporation) exhibited either the pump-state with resting PD of −151 ± 12 mV (6 cells, 12 profiles) or the background-state with PD of −108 ± 12 mV (7 cells, 10 profiles). The data are shown in Fig. 3, using the same conventions as in Fig. 2. In this group of data the background-state shows the drop of current at −20 mV caused by excitation. Note that the total background-state current and conductance are slightly larger than the fitted background current and conductance of the pump-state (Fig. 3*b* and *c*, PDs more positive than −100 mV).

Both the pump- and the background-state exhibited inward rectification and the modeled i_{irc} is shown for each state (thick and thin dashed lines in 3*b* and *c*). Note that the g_{irc} (background-state) is higher than the g_{irc} (pump-state). This is reflected by the parameters in Table 2: the background rectifier was fitted with a less hyperpolarized V_{50}, greater $N_K P_K$, and z_g of 2. As it was not possible to obtain many data sets with well-defined inward rectifiers at higher salinity (*see* Methods), this was a good opportunity to fit equations (3) and (4). Fig. 4 shows the background *I/V* profile replotted on a smaller scale to show the full data set. A small pump current contribution is shown in 4*b*. The pump current components of similar magnitude were fitted to the background-states at other salinities. The parameters are given in Table 2.

The cells in 0.4 SW and 0.5 SW show about 50% chance for either pump- or background-state. However,

Table 2. Model parameters for steady-state I/V profiles in a range of salinities

Data set	Pump parameters				i_{orc}			i_{irc}			$g_{background}$	V_P*	V_R*
	k^o_{io}	k^o_{oi}	κ_{io}	κ_{oi}	k_1		k_2	c_1		c_2			
	sec^{-1}										$S \cdot m^{-2}$	mV	mV
Chara													
Plasmalemma Blatt, Beilby & Tester, 1990 pH 7.5	5920	0.11	0.085	102							~0.3	−457	−230
Both membranes Beilby & Walker, 1996	5000	1.05	0.1	23	26		1.5	46		15	0.15	−349	−217
					V_{50}	N_KP_K	z_g	V_{50}	N_KP_K	z_g			
					mV	$m^3 \cdot sec^{-1} \times 10^{-7}$		mV	$m^3 \cdot sec^{-1} \times 10^{-7}$				
Lamprothamnium													
Pump-state 0.2 SW 6 cells, 16 profiles	4000	0.8	0.5	175	−65	50.0	2	−375	0.75	1	0.5	−360	−219
Pump-state 0.4 SW 6 cells, 7 profiles	3000	0.5	0.5	130	50	5.0	2	−390	5.0	1	2.15	−366	−161
Background-state 0.4 SW 7 cells, 12 profiles	3000	0.5	0.5	8							2.2	−289	−107
Pump-state 0.5 SW 6 cells, 12 profiles	7000	0.5	0.5	380				−291	5.0	1	6.5	−407	−152
Background-state 0.5 SW 7 cells, 10 profiles	7000	0.5	0.5	20				−268	10.0	2	7.6	−333	−105
Pump-state full SW 8 cells, 13 profiles	11,000	0.5	0.5	550	90	0.5	1	−370	50.0	1	16.0	−428	−137
Background-state full SW 3 cells, 5 profiles	11,000	0.5	0.5	50	90	0.02	1				22.0	−368	−104

* V_P is pump reversal PD; V_R is resting PD.

the cells in the most dilute medium (0.2 SW) were found only in pump-state and, rather unexpectedly, the cells in full SW also exhibited a preference for the pump-state. The pump-state of PD −137 ± 12 mV (8 cells, 13 profiles) and background-state with PD of −104 ± 12 mV (3 cells, 5 profiles) are shown in Fig. 5, using the same conventions as in Fig. 2. The parameters are given in Table 2. The dip in the pump-state current at 0 PD is due to excitation. The total background-state conductance in this medium is greater than the fitted background conductance in the pump-state (Fig. 5*c*).

The overall trends of the fitted pump and background currents with salinity are summarized in Fig. 6. The total currents (Fig. 6*a*) and the total conductances (Fig. 6*c*) are shown as continuous lines. The pump and the background currents are shown (Fig. 6*b*) as in Figs. 1–5. The media are numbered "1" for 0.2 SW to "4" for full SW. The background conductance increased 32-fold, from 0.5 to 16.0 $S \cdot m^{-2}$, as the medium ranged from 0.2 SW to full SW (Fig. 6*c*). Note, however, that the reversal PD for the background current remained at −100 mV. The peak conductance of the pump (located between −140 and −190 mV) remained near 1 $S \cdot m^{-2}$ from 0.2 SW to 0.4 SW, but increased to ~4 $S \cdot m^{-2}$ in 0.5 SW and further to ~5 $S \cdot m^{-2}$ in full SW (Fig. 6*c*). The cells have a remarkable capacity to maintain a pump-state against the high background conductance in very saline media (full SW).

Hypertonic Effect

Three of the very hyperpolarized cells growing in 0.2 SW were exposed to hypertonic medium (0.4 SW), giving similar responses. Initially, the cells were all in

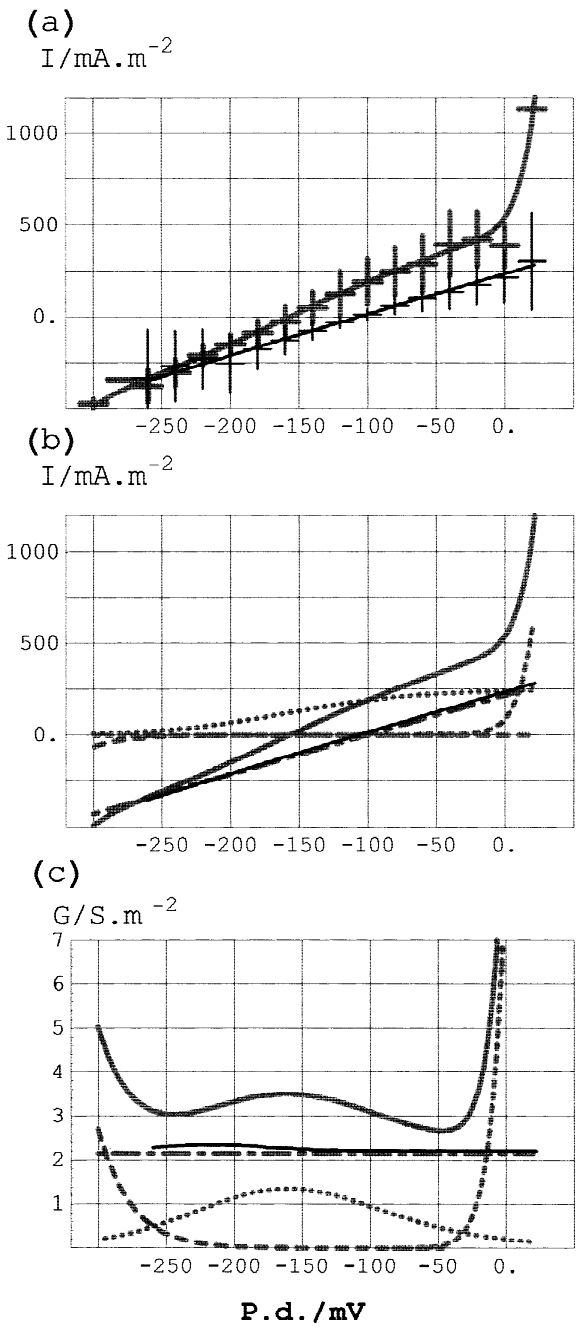

Fig. 2. (*a*) A set of 6 cells, 7 profiles, in pump-state (thick error bars) and a set of 7 cells, 12 profiles, in background-state (thin error bars) grown in 0.4 SW. The data have been gathered into 20 mV slots (horizontal error bars) and the standard errors are shown as the vertical bars. The cells in pump-state did show some excitability, which resulted in smaller current amplitude at 0 PD. The cells in background-state were not excitable. (*b*) The transport systems constituting the *I/V* profile: ····· the pump, — - — - — - the background current, ------ the inward rectifier i_{irc}, - - - - the outward rectifier i_{orc}. The thin continuous line shows the total modeled background current. For the mathematical forms, *see* Methods. The parameter values can be found in Table 2. (*c*) The corresponding *G/V* profiles. The thin continuous line shows the total background conductance.

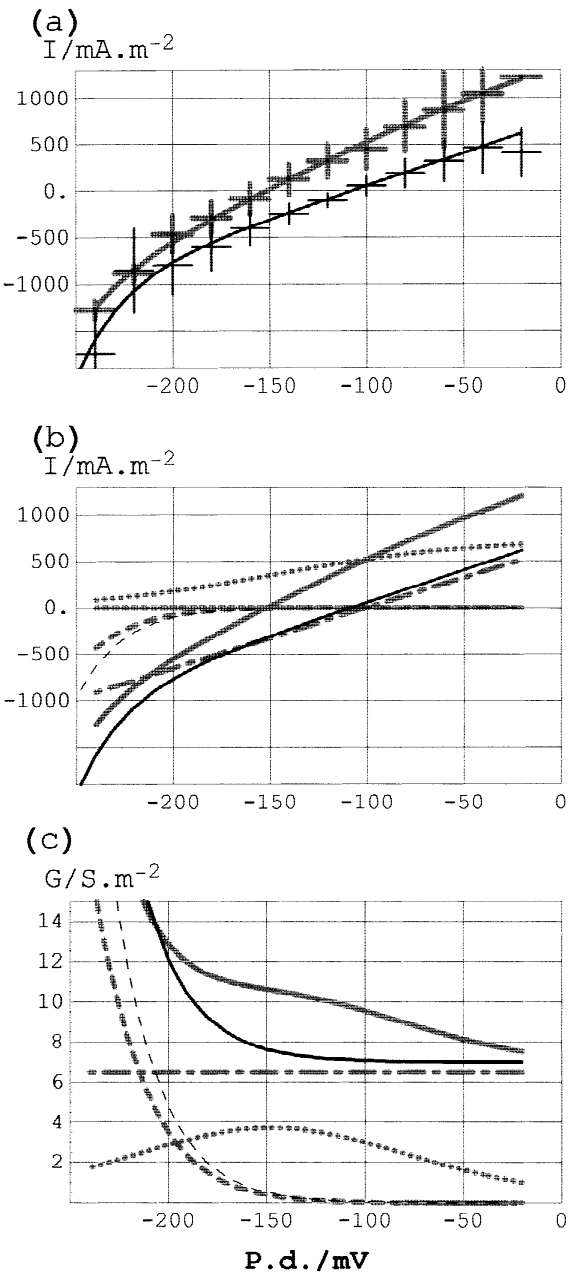

Fig. 3. (*a*) A set of 6 cells, 12 profiles, in pump-state (thick error bars) and a set of 7 cells, 10 profiles, in background-state (thin error bars) grown in 0.5 SW. The cells in background-state did show some excitability, which resulted in smaller current amplitude at −20 mV. The cells in pump-state were not excitable in this PD window. The data have been gathered into 20 mV slots (horizontal error bars) and the standard errors are shown as the vertical bars. The lines represent the *I/V* profiles generated by the model as in Fig. 2. The resting PDs are given in Table 2. (*b*) The transport systems constituting the pump *I/V* profile: ····· the pump, — - — - — the background current, ------- the inward rectifier i_{irc}, - - - - the outward rectifier i_{orc}. The thin continuous line shows the total modeled background current. For the mathematical form, *see* Methods. The parameter values can be found in Table 2. (*c*) The corresponding *G/V* profiles. The thin continuous line shows the total background conductance.

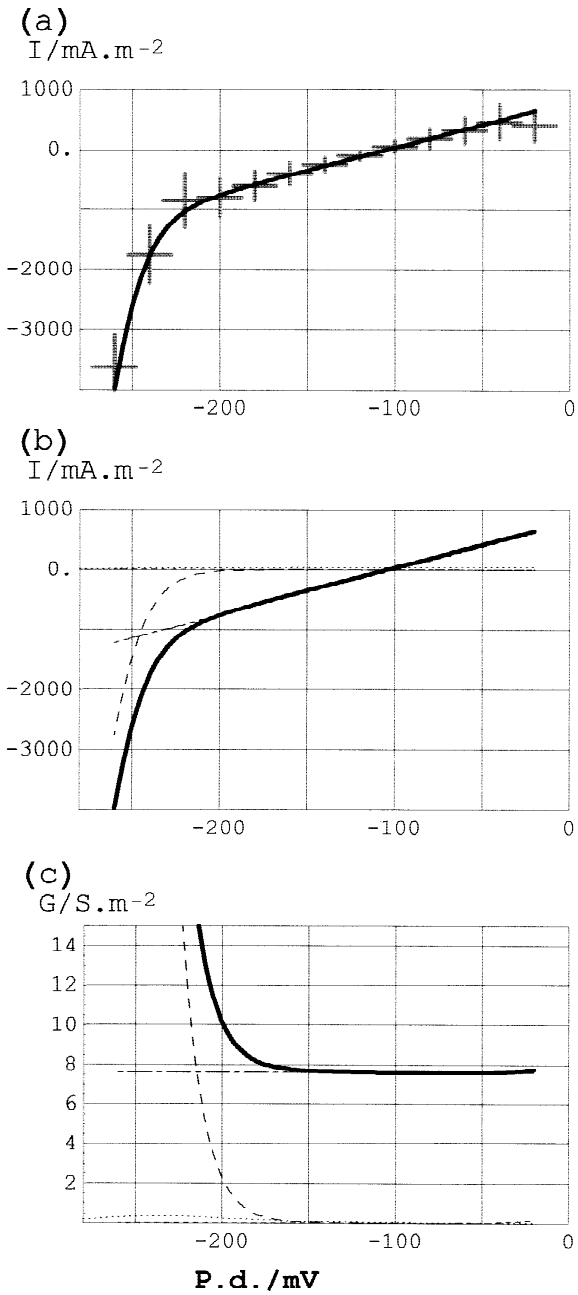

Fig. 4. (*a*) The total background-state current from Fig. 3 replotted to show the inward rectifier. (*b*) The transport systems constituting the *I/V* profile: ····· the pump, — - — - — the background current, ------- the inward rectifier i_{irc}, - - - - the outward rectifier i_{orc}. (*c*) The corresponding *G/V* profiles. The continuous lines represent the total *I/V* profiles generated by the model. The resting PDs are given in Table 2.

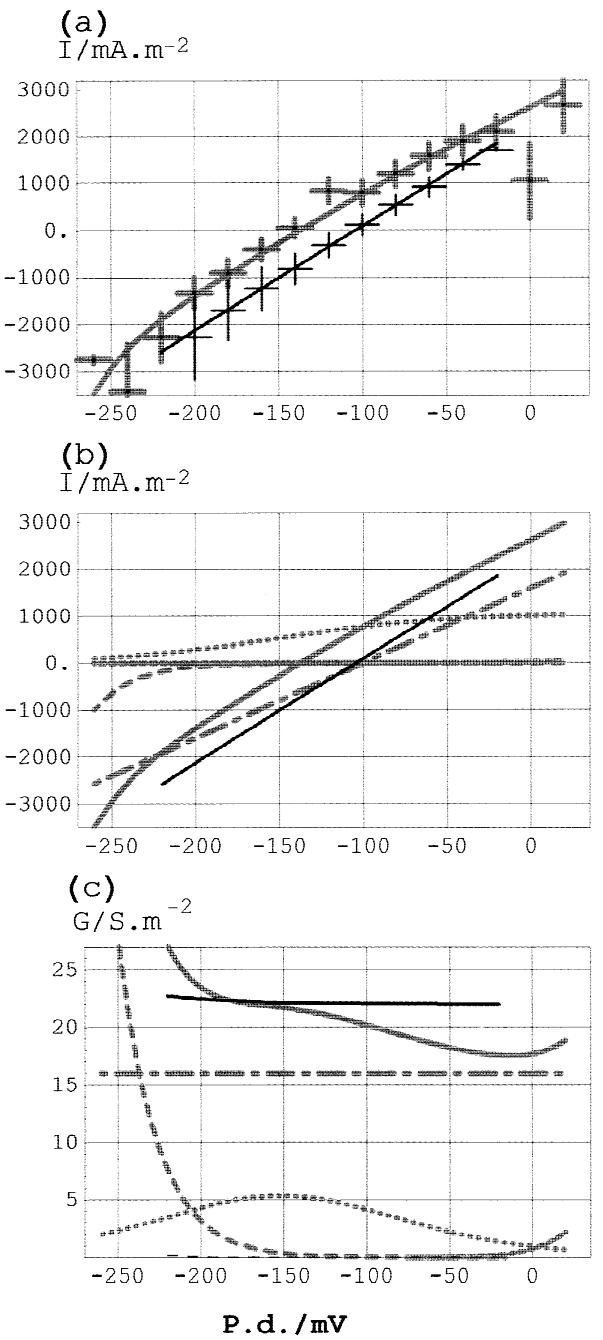

Fig. 5. (*a*) A set of 8 cells, 13 profiles, in pump-state (thick error bars) and a set of 3 cells, 5 profiles, in background-state (thin error bars) grown in full SW. The data have been gathered into 20 mV slots (horizontal error bars) and the standard errors are shown as the vertical bars. The lines represent the *I/V* profiles generated by the model as in Fig. 2. The resting PDs are given in Table 2. (*b*) The transport systems constituting the total pump-state *I/V* profile: ····· the pump, — - — - — the background current, ------- the inward rectifier i_{irc}, - - - the outward rectifier i_{orc}. The thin continuous line shows the total model background current. For the mathematical forms, *see* Methods. The parameter values can be found in Table 2. (*c*) The corresponding *G/V* profiles. The thin continuous line shows the total background conductance.

pump-state. The resting PD of these cells was the most negative we have encountered in *Lamprothamnium* (−219 ± 12 mV). A typical hypertonic sequence is shown in Fig. 7. The steady state *I/V* profile is shown as the thick gray line (7*a*). Upon introduction of the hyper-

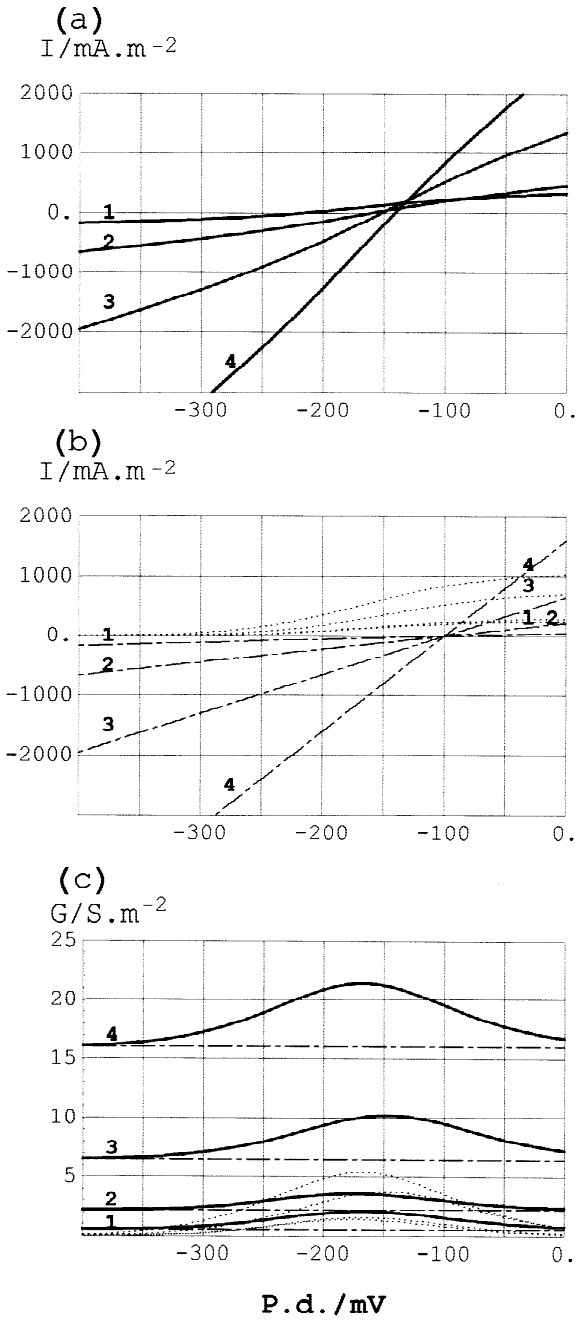

Fig. 6. (*a*) Summary of the *Lamprothamnium I/V* profiles at steady state in media of different salinity: "1" stands for 0.2 SW, "2" stands for 0.4 SW, "3" stands for 0.5 SW and "4" stands for full SW. (*b*) Only the pump current ····· and the background current — - — - — are shown. (*c*) The corresponding *G/V* profiles.

tonic medium no obvious electrical response was discernible from 0 to 3 min. There was no evidence of plasmolysis, and no effect on cytoplasmic streaming. Between 4 and 5 min (curve 1, violet blue line), the cell depolarized by a small amount (<4 mV). For the next 20 min, the cells hyperpolarized very slowly, at rates of 1.2

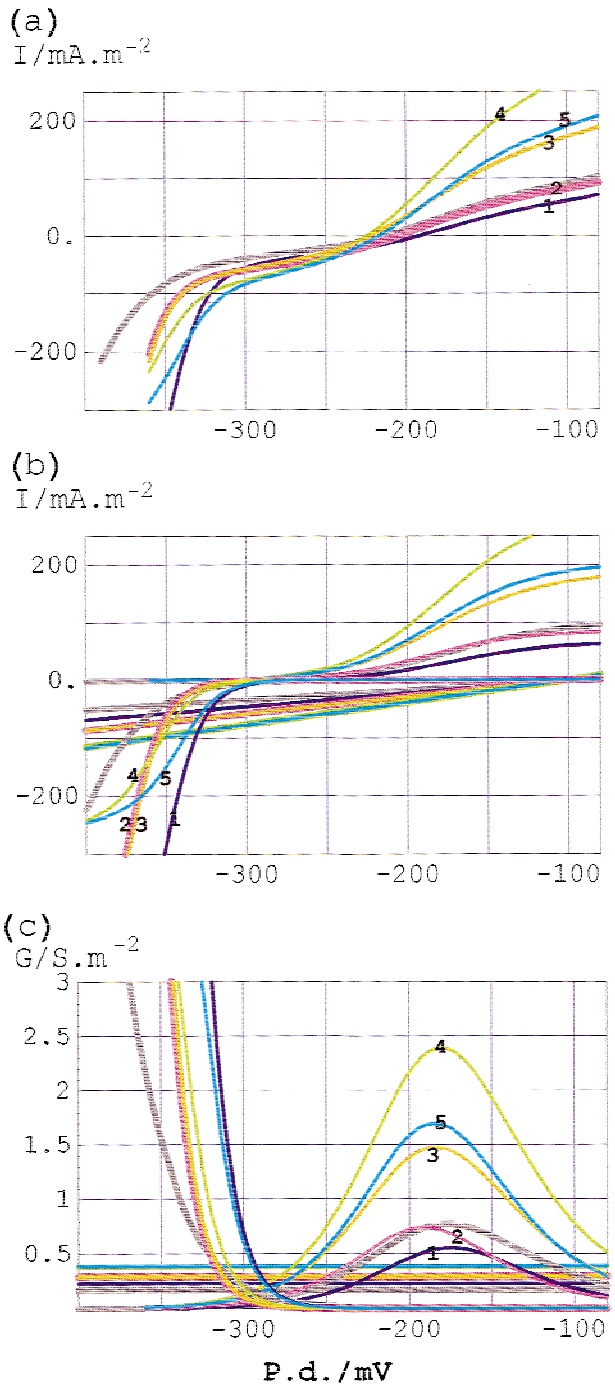

Fig. 7. (*a*) Response of a 0.2 SW cell to hypertonic challenge. The steady-state *I/V* profile is depicted by a thick gray line. The successive profiles in hypertonic solution are signified by lines of different color: 5 min (curve *1*, violet blue), 21 min (curve *2*, pink red), 41 min (curve *3*, orange), 2 hr 34 min (curve *4*, yellow green) and 3 hr 30 min (curve *5*, light blue). (*b*) The three transport systems, used to model the data: the pump, the background current and the inward rectifier. Same colors as in (*a*) have been employed. The background currents *2* and *3* and the background currents *4* and *5* overlap. The inward rectifier currents *2* and *3* also overlap. The parameter values can be found in Table 3. (*c*) The corresponding *G/V* profiles for the three transporters.

Table 3. Hypertonic sequence

Data set	Pump parameters				i_{orc}			i_{irc}			$g_{background}$	V_P*	V_R*
	k^o_{io}	k^o_{oi}	κ_{io}	κ_{oi}	V_{50}	$N_K P_K$	z_g	V_{50}	$N_K P_K$	z_g			
	sec^{-1}				mV	$m^3 \cdot sec^{-1} \times 10^{-7}$		mV	$m^3 \cdot sec^{-1} \times 10^{-7}$		$S \cdot m^{-2}$	mV	mV
Steady-state 0.2 SW stats: 6 cells, 17 profiles	4000	0.8	0.5	159	−65	50.0	2	−375	0.75	1	0.5	−359	−219
Steady-state 0.2 SW	2800	1.5	0.5	55				−414	2.0	1	0.17	−308	−215
Hyper exposure (1) 5 min 0.4 SW	2700	2.0	0.5	35				−351	1.5	2	0.23	−288	−192
Hyper exposure (2) 21 min 0.4 SW	6000	2.5	0.5	45				−376.5	1.5	2	0.29	−309	−204
Hyper exposure (3) 41 min 0.4 SW	7000	3.2	0.5	100				−375	1.5	2	0.29	−327	−222
Hyper exposure (4) 2 hr 34 min 0.4 SW	11000	6.0	0.5	160				−355	0.55	2	0.385	−330	−220
Hyper exposure (5) 3 hr 30 min 0.4 SW	9900	5.0	0.5	108				−340	0.56	2	0.39	−324	−222

The fit parameters are given for an average of 6 cells in 0.2 SW (row 1), single cell in 0.2 SW (row 2) and response of this cell to hypertonic medium 0.4 SW after 5 min (1), 21 min (2), 41 min (3), 2 hr 34 min (4), and 3 hr 30 min (5). For the meaning of various parameters, *see* Methods.
* V_P is pump reversal PD; V_R is resting PD.

to 2 mV per min. The successive profiles in hypertonic solution are signified by dashing of increasing length, starting at 21 min (curve 2, pink red), 41 min (curve 3, orange), 2 hr 34 min (curve 4, yellow-green) and 3 hr 30 min (curve 5, light blue). The modeled pump-, background- and inward-rectifier currents are shown in 7*b* and the conductances in 7*c*. The parameters are listed in Table 3.

Discussion

The Steady-State Transporters as a Function of Salinity

The Background Current

The steady-state membrane conductance increases from 2–22 $S \cdot m^{-2}$ as the salinity increases from 0.2 to full SW (see Figs. 1–5). Our modeling confirms that the major component of this increase is the background current (*see* Fig. 6). The reversal PD of the modeled background current remains at −100 mV. The *I/V* curves from the cells in the background-state support the model. The lack of response of the reversal PD to considerable changes of Na^+ and Cl^- concentrations (*see* Table 1), suggests that neither of these ions contribute substantially to background current. The linear *I/V* profile and fast response to PD change points to voltage-independent channels as transporters of the background current (*VICs*, see Amtmann & Sanders, 1999 and references therein). While *VICs* in glycophytes exhibit low Na^+-K^+ discrimination (Amtmann & Sanders, 1999), the background channels in salt-tolerant *Lamprothamnium* seem to have very low Na^+ permeability. This adaptation may facilitate survival in high salt media. The two ions likely to carry the background current are K^+ and H^+, but even the K^+ concentration changes sufficiently to depolarize the reversal PD by about 50 mV in the full range of the media tested (*see* Table 1). Yao and Bisson (1993) found that another salt-tolerant charophyte, *Chara longifolia*, exhibits increased membrane conductance in more saline media. They suggest that passive proton conductance rises with rising salinity, as the area of alkaline extracellular bands was observed to grow. Our cells did not appear to band, but we will investigate this hypothesis by exposing the cells to a range of pH at different salinities. This treatment will affect the proton pump as well (Beilby, 1984), but with the aid of modeling, the behavior of the reversal PD of the background current will be isolated. The effect of $[K^+]_o$ on the background current and the K^+ state is being investigated in a separate study. Preliminary results indicate a shift of the reversal PD of the background current with high $[K^+]_o$, but detailed modeling will be necessary to quantify this change.

Whatever ions are involved, physical effects from increasing salinity would be expected to contribute, in-

cluding electrostatic screening by the impermeant ions at the mouth of the ion channels, enabling higher conductivity for the permeant ions (Läuger, 1976). This hypothesis will be tested by replacing the high NaCl by an appropriate concentration of sorbitol or some other uncharged solute. When the identity of the ions carrying the background current is revealed, this current will be also fitted by the GHK model.

The Proton Pump

The peak pump conductance increased about five times for salinity change from 0.2 SW to full SW (*see* Fig. 6*c*). The position of the peak with respect to the membrane PD did not change appreciably with salinity of the medium. It is slightly depolarized compared to that of *Chara* at the same pH_o (Beilby, 1984). Table 2 shows that the pump parameters that change with increasing salinity are k^o_{io} and κ_{oi}. The effects of increase in these two parameters on the shape of the model *I/V* relationship are described by Beilby and Walker (1996). The k^o_{io} is a reaction constant for the charge transit across the membrane, while κ_{oi} is a reaction constant which lumps voltage-independent processes, ATP-, ADP-, P_i and transported ion binding and debinding steps (Blatt, Beilby & Tester, 1990). The increase in k^o_{io} produces movement along the V axis of the pump *I/V* curve, while the increase in κ_{oi} is associated with greater amplitude of positive current. These two adaptations partially counteract the larger conductance of the background current in high salinity to hold the resting PD negative. The higher rate of pumping is likely to be energy-costly and this is reflected by the morphology of the plants: large plants with long cells in low salinity, small plants with short cells in full seawater. The higher proton pumping rate was also observed in other plant systems under hypertonic stress: *Chara longifolia* (Yao, Bisson & Brzezicki, 1992), leaf segments of *Senecio mikanioides* Otto (Reinhold et al., 1984), cultured cells of *Arabidopsis thaliana* L. (Curti et al., 1993) and bean mesophyll cells (Shabala et al., 2000).

Hypertonic Regulation

The Proton Pump

The response of the proton pump when the medium was stepped up from 0.2 SW to 0.4 SW, is shown in Fig. 7*b*. After five min, when the cells transiently depolarized (by < 4 mV) the pump current actually dropped via a very small drop in k^o_{io} and a larger drop in κ_{io}. After 20 min, as the cell gradually hyperpolarized, k^o_{oi} increased, and came to a maximum after 2.5 hr in the hypertonic medium. This maximal rate was as high as in full SW (*compare* Tables 1 and 2). The rate constant κ_{oi} also came to a maximum at this time, but the value was appropriate for the 0.4 SW. The reverse constant for the charged step, k^o_{oi}, also increased—this was not observed in the steady-state response to increasing salinity.

Lamprothamnium succinctum displayed greater hyperpolarization by ~50 mV (Okazaki et al., 1984; Okazaki & Tazawa, 1990) than observed in the present study (~5 to 20 mV), but this was over a far longer time-course (~20 hr). Moreover, the 0.2 SW cells were already substantially hyperpolarized, with exceptionally negative PDs (~ −219 mV), even before the hypertonic exposure (*see* Fig. 1*a*). Other researchers (*see* Beilby and Shepherd, 1996) have reported PDs for *Lamprothamnium* in the range of −180 mV. We may be seeing the pump running at close to its limit. The hyperpolarization found in higher plant cells exposed to hypertonic stress is in a similar range: 20 mV (bean mesophyll cells, Shabala et al., 2000), 50 mV (broadbean mesocarp cells, Li & Delrot, 1987), 70 mV (sugar beet tap root cells, Kinraide & Wyse, 1986).

The Inward Rectifier

The inward rectifier was modeled by the GHK equation (*see* Methods). While the i_{irc} might have not reached full equilibrium at each PD level, the time dependence of the fast current relaxation remained constant throughout the hypertonic experiment. The most interesting finding from Fig. 7 and Table 3 is the prompt activation of the inward rectifier in the first 5 min of exposure to the hypertonic solution. This first hypertonic membrane profile was fitted with V_{50} becoming more positive by 60 mV, compared to steady state, and the gating charge, z_g, increasing from 1 to 2. If z_g was kept at 1, the greatly increased slope of the current could only be achieved by an unrealistic increase in $N_K P_K$. The gating charge, $z_g = 2$, was also fitted to background-state cells in 0.5 SW (Fig. 4), but most cells in steady-state exhibited a more gradual current rise with hyperpolarization, fitted with $z_g = 1$ (*see* Table 2). While it is not known what might cause such a change in the steady-state, rapid and unexpected increases in the slope of the rectifier current have been observed in many of our experiments, often with fatal consequences for the cell under voltage-clamp conditions. While long time-dependence of the inward rectifier needs more study, it is also possible that the K^+ influx follows some long-term oscillatory behavior (Gradmann & Hoffstadt, 1998).

The Turgor-Sensing Mechanism

Table 3 shows that both the background current and the proton pump responded rather slowly to the hypertonic challenge, being effectors rather than detectors of the medium concentration change. The speed and magni-

tude of the change in the K^+ inward rectifier (Fig. 7) make it a more likely candidate for a hypertonic turgor-sensing mechanism. This finding is in agreement with conclusions of Shabala et al. (2000), who found no increase in proton efflux, for hypertonic exposure of bean mesophyll cells in a medium lacking K^+. Blatt (1991) reports that $[K^+]_o$ does not affect the parameters of the K^+ inward rectifier of guard cells, but the amplitude of the currents becomes vanishingly small below 1 mM. Consequently, an increase in K^+ influx is necessary to stimulate the proton pump upon hypertonic exposure. Liu and Luan (1998) also consider K^+ channels to be the turgor sensors in guard cells. In our future work we will investigate how the inward K^+ rectifier senses the turgor drop and how it influences the H^+ pump.

References

Amtmann, A., Sanders, D. 1999. Mechanisms of Na^+ uptake by plant cells. *Adv. Bot. Res.* **29:**75–112

Ashraf, M. 1994. Breeding for salinity tolerance in plants. *Crit. Rev. Plant Sci.* **13:**17–42

Baldauf, S.L., Manhart, J.R., Palmer, J.D. 1990. Different fates of the chloroplast tufA gene following its transfer to the nucleus in green algae. *Proc. Nat. Acad. Sci. USA* **87:**5317–5321

Beilby, M.J. 1984. Current-voltage characteristics of the proton pump at *Chara* plasmalemma: I. pH dependence. *J. Membrane Biol.* **81:**113–125.

Beilby, M.J. 1990. Current-voltage curves for plant membrane studies: A critical analysis of the method. *J. Exp. Bot.* **41:**165–182

Beilby, M.J., Mimura, T., Shimmen, T. 1997. Perfusion: A critical analysis of the method. *J. Exp. Bot.* **48:**157–72

Beilby, M.J., Shepherd, V.A. 1996. Turgor regulation in *Lamprothamnium papulosum*: I. I/V analysis and pharmacological dissection of the hypotonic effect. *Plant, Cell, Environ.* **19:**837–847

Beilby, M.J., Walker, N.A. 1981. Chloride transport in *Chara*: I. Kinetics and current-voltage curves for a probable proton symport. *J. Exp. Bot.* **32:**43–54

Beilby, M.J., Walker, N.A. 1996. Modeling the current-voltage characteristics of *Chara* membranes: I. The Effect of ATP removal and zero turgor. *J. Membrane Biol.* **149:**89–101

Bisson, M.A., Kirst, G. 1980. *Lamprothamnium*, a euryhaline charophyte II. Osmotic relations and membrane potential at steady state. *J. Exp. Bot.* **31:**1237–1244

Blatt, M.R. 1991. Ion channel gating in plants: Physiological implications and integration for stomatal function. *J. Membrane Biol.* **124:**95–112

Blatt, M.R. 1999. Reassessing roles for Ca^{2+} in guard cell signaling. *J. Exp. Bot.* **50:**989–999

Blatt, M.R., Beilby, M.J., Tester, M. 1990. Voltage dependence of the *Chara* proton pump revealed by current-voltage measurement during rapid metabolic blockade with cyanide. *J. Membrane Biol.* **114:**205–223

Blumwald, E., Gelli, A. 1997. Secondary inorganic ion transport at the tonoplast. *Adv. Bot. Res.* **25:**401–417

Bremer, K., Humphries, C.J., Mishler, B.D., and Churchill, S.P. 1987. On cladistic relationships in green plants. *Taxon.* **36:**339–349

Cerda, A., Pardines, J., Botella, M.A., Martinez, V. 1995. Effect of potassium on growth, water relations, and the inorganic and organic solute contents for two maize cultivars grown under saline conditions. *J. Plant Nutrition* **18:**839–851

Chamberlin, M.E., Strange, K. 1989. Anisosmotic cell volume regulation: a comparative review. *Amer. J. Physiol.* **257:**C159–C173

Colombo, R., Cerana, R. 1992. Inward rectifying K^+ channels in the plasma membrane of *Arabidopsis thaliana*. *Plant Physiol.* **77:**1130–1135

Cosgrove, D.J., Hedrich, R. 1991. Stretch-activated chloride, potassium, and calcium channels coexisting in plasma membranes of guard cells of *Vicia faba* L. *Planta* **186:**143–153

Curti, G., Massardi, F., Lado, P. 1993. Synergistic activation of plasma membrane H^+-ATPase in *Arabidopsis thaliana* cells by turgor decrease and by fusicoccin. *Physiologia Plantarum* **87:**592–600

Findlay, G.P., Tyerman, S.D., Garril, A., Skerrett, M. 1994. Pump and K^+ inward rectifiers in the plasmalemma of wheat root protoplasts. *J. Membrane Biol.* **139:**103–116

Gradmann, D., Hoffstadt, J. 1998. Electrocoupling of ion transporters in plants: Interaction with internal ion concentrations. *J. Membrane Biol.* **166:**51–59

Gunning, B.E.S., Schwartz, O.M. 1999. Confocal microscopy of thylakoid autofluorescence in relation to origin of grana and phylogeny in green algae. *Aust. J. Plant Physiol.* **26:**695–708

Hansen, U.-P., Gradmann, D., Sanders, D., Slayman, C.L. 1981. Interpretation of current-voltage relationships for "active" ion transport systems: I. Steady-state reaction-kinetic analysis of class-I mechanisms. *J. Membrane Biol.* **63:**165–190

Hedrich, R., Busch, H., Raschke, K. 1990. Ca^{++}- and nucleotide-dependent regulation of voltage-dependent anion channels in the plasma membrane of guard cells. *EMBO J.* **9:**3889–3892

Hope, A.B., Walker, N.A. 1975. The Physiology of Giant Algal Cells. Cambridge University Press, London

Hu, Y., Schmidhalter, U. 1998. Spatial distributions of inorganic ions and sugars contributing to osmotic adjustment in the elongating wheat leaf under saline conditions. *Aust. J. Plant Physiol.* **25:**591–597

Kerr, R.A. 1998. Sea-floor dust shows drought felled Akkadian empire. *Science* **279:**325–326

Kinraide, T.B., Wyse, R.E. 1986. Electrical evidence for turgor inhibition of proton extrusion in sugar beet taproot. *Plant Physiol.* **82:**1148–1150

Kourie, J.I., Findlay, G.P. 1990. Ionic currents across the plasmalemma of *Chara inflata* cells. I. Osmotic effects of sorbitol on K^+, Cl^- and leak currents. *J. Exp. Bot.* **41:**141–150

Läuger, P. 1976. Diffusion-limited ion flow through pores. *Biochim. Biophys. Acta* **455:**493–509

Li, Z., Delrot, S. 1987. Osmotic dependence of the transmembrane potential difference of broadbean mesocarp cells. *Plant Physiol.* **84:**895–899

Liu, K., Luan, S. 1998. Voltage-dependent K^+ channels as targets of osmosensing in guard cells. *The Plant Cell* **10:**1957–1970

Manhart, J.R., Palmer, J.D. 1990. The gain of two chloroplast tRNA introns marks the green algal ancestors of land plants. *Nature* **345:**268–270

McCulloch, S.R., Beilby, M.J. 1997. The electrophysiology of plasmolysed cells of *Chara australis*. *J. Exp. Bot.* **48:**1383–1392

Okazaki, Y., Shimmen, T., Tazawa, M. 1984. Turgor regulation in brackish charophyte, *Lamprothamnium succinctum* II. changes in K^+, Na^+, and Cl^- concentrations, membrane potential and membrane resistance during turgor regulation. *Plant Cell Physiol.* **25:**573–581

Okazaki, Y., Tazawa, M. 1990. Calcium ion and turgor regulation in plant cells. *J. Membrane Biol.* **114:**189–194

Okazaki, Y. 1993. *in* Giant Cells of the Characeae, International Seminar House, Otsu, Japan, September 4–6, pp. 33

Pickard, B.G., Ding, J.P. 1993. The mechanosensory calcium-selective

ion channels—key component of a plasmalemmal control centre. *Aust. J. Plant Physiol.* **20:**439–459

Reinhold, L., Seiden, A., Volokita, M. 1984. Is modulation of the rate of proton pumping a key event in osmoregulation? *Plant Physiol.* **75:**846–849

Sanders, D. 1980. Control of Cl^- influx in *Chara* by cytoplasmic Cl^- concentration. *J. Membrane Biol.* **52:**51–60

Shabala, S., Babourina, O., Newman, I. 2000. Ion-specific mechanisms of osmoregulation in bean mesophyll cells. *J. Exp. Bot.* **51:**1243–1253

Shepherd, V.A., Beilby, M.J., Heslop, D. 1999. Ecophysiology of the hypotonic response in the salt-tolerant alga *Lamprothamnium papulosum*. *Plant, Cell Environ.* **22:**333–346

Suarez, N., Sobrado, M.A., Medina, E. 1998. Salinity effects on the leaf water relations components and ion accumulation patterns in *Avicennia germinans* L. seedlings. *Oecologia* **114:**299–304

Thiel, G., Blatt, M.R., Fricker, M.D., White, I.R., Millner, P. 1993. Modulation of K^+ channels in *Vicia* stomatal guard cells by peptide homologs to the auxin-binding protein C terminus. *Proc. Natl. Acad. Sci. USA* **90:**11493–11497

Tyerman, S.D., Findlay, G.P., Paterson, G.J. 1986a. Inward membrane current in *Chara inflata*. I. A voltage- and time-dependent component. *J. Membrane Biol.* **89:**139–152

Tyerman, S.D., Findlay, G.P., Paterson, G.J. 1986b. Inward membrane current in *Chara inflata*. I. Effects of pH, Cl^--channel blockers and NH^+_4, and significance for the hyperpolarized state. *J. Membrane Biol.* **89:**153–161

Tyerman, S.D., Skerrett, M., Garrill, A., Findlay, G.P., Leigh, R.A. 1997. Pathways for the permeation of Na^+ and Cl^- into protoplasts derived from the cortex of wheat roots. *J. Exp. Bot.* **48:**459–480

Winter, U., Soulie-Marsche, I., and Kirst, G.O. 1996. Effects of salinity on turgor pressure and fertility in *Tolypella* (Characeae). *Plant Cell Environ.* **103:**197–203

Yao, X., Bisson, M.A. 1993. Passive proton conductance is the major reason for membrane depolarization and conductance increase in *Chara buckellii* in high salt condition. *Plant Physiol.* **103:**197–203

Yao, X., Bisson, M.A., Brzezicki, L.J. 1992. ATP-driven proton pumping in two species of *Chara* differing in salt tolerance. *Plant Cell Environ.* **15:**199–210